
PICTORIAL ESSAY

Application of Zero Echo Time Magnetic Resonance Angiography in Neuroimaging: A Pictorial Essay

WC Law¹, BMH Lai¹, CY Cheung², KT Wong¹, JM Abrigo¹

¹*Department of Imaging and Interventional Radiology, The Chinese University of Hong Kong, Prince of Wales Hospital, Hong Kong SAR, China*

²*Department of Radiology, North District Hospital, Hong Kong SAR, China*

INTRODUCTION

Cerebrovascular malformations are characterised by abnormal communications between high-velocity-flow arteries and low-velocity-flow veins and venous sinuses in the brain. Such gradient differences put cerebrovascular malformations at risk for intracranial haemorrhage, which is often associated with significant morbidity and mortality. Digital subtraction angiography (DSA) is the gold standard for imaging assessment because of its high spatial resolution and dynamic information. However, it is an invasive procedure and uses a high radiation dose, making it less than ideal for screening and surveillance purposes.

Magnetic resonance angiography (MRA) with time-of-flight (TOF) technique is widely used as a non-invasive investigation to diagnose or follow up patients with

cerebrovascular malformations. It does not require contrast medium and utilises the inflow effect for generation of images of vessels.¹ However, there are some limitations of this technique. It is influenced by haemodynamics; for instance, in areas with complex vessel direction, such as the internal carotid artery (ICA) siphon, the images may be suboptimal with heterogeneous flow signal. It may also depict artefactual flow signal in the cavernous sinus in patients without carotid cavernous fistula (CCF)² or in the dural venous sinuses in patients without dural arteriovenous fistula (AVF).¹ Magnetic susceptibility artefacts and radiofrequency shielding often lead to difficulty in evaluation of patients who have undergone previous interventions such as coil embolisation and stenting.

In clinical practice, contrast-enhanced MRA may be

Correspondence: Dr WC Law, Department of Imaging and Interventional Radiology, Prince of Wales Hospital, The Chinese University of Hong Kong, Hong Kong SAR, China
Email: lwc926@ha.org.hk

Submitted: 21 March 2023; Accepted: 29 September 2023.

Contributors: WCL and JMA designed the study. WCL acquired data. All authors analysed the data. WCL and JMA drafted the manuscript. All authors critically revised the manuscript for important intellectual content. All authors had full access to the data, contributed to the study, approved the final version for publication, and take responsibility for its accuracy and integrity.

Conflicts of Interest: All authors have disclosed no conflicts of interest.

Funding/Support: This study received no specific grant from any funding agency in the public, commercial, or not-for-profit sectors.

Data Availability: All data generated or analysed during the present study are available from the corresponding author on reasonable request.

Ethics Approval: This study was approved by the Joint Chinese University of Hong Kong–New Territories East Cluster Clinical Research Ethics Committee, Hong Kong (Ref No.: 2022.396). Informed patient consent was waived by the Committee due to the retrospective nature of the study.

Acknowledgement: The authors thank Mr William Kin-ming Kwong, Senior Radiographer in the Department of Imaging and Interventional Radiology in Prince of Wales Hospital, for his technical support on magnetic resonance imaging protocols.

additionally performed for clarification. The multiphase acquisition slightly increases the complexity of interpretation but allows dynamic visualisation of early venous drainage, confirming arteriovenous shunting. It does require intravenous administration of gadolinium contrast, which is contraindicated in patients with renal impairment, and also makes it less than ideal for surveillance screening purposes. In addition, the spatial resolution of contrast-enhanced MRA is usually inferior to that of TOF MRA.

Zero echo time (ZTE) MRA, also called silent MRA, is a relatively new technique, which combines ultrashort echo time (0.006 ms) with arterial spin labelling (ASL). The ASL technique uses magnetically labelled blood as endogenous contrast, and the final angiographic image is generated by subtraction of pre- from post-labelled images, achieving background suppression. ZTE has minimal magnetic susceptibility artefact and the ASL technique improves the detection of low-flow signal.

Several studies have reported the usefulness of silent MRA for the characterisation of cerebrovascular diseases (atherosclerotic steno-occlusions, moyamoya disease, and arteriovenous malformations [AVMs])³ and follow-up of treated aneurysms.⁴⁻⁶ It has also recently been reported as being useful for dural AVFs and indirect CCFs.^{7,8} In our experience, it is helpful for identification and follow-up of different kinds of cerebrovascular malformations, as it facilitates depiction of 'arterialised' veins/venous sinuses. Here we present a pictorial essay of our experience, illustrating the applicability of ZTE MRA in our clinical practice.

Study Population

The relevant MRA scans were retrospectively retrieved from 1 January 2017 to 31 July 2022 using keyword search of radiology reports in the Radiology Information System, a system widely used by every radiology department in Hong Kong. All patients with ZTE MRA acquired for the evaluation or follow-up of vascular

malformations with positive imaging findings were included. Patients with cerebrovascular abnormalities other than AVM and AVF were excluded. The corresponding MRI images and DSA studies were also reviewed.

Zero Echo Time Magnetic Resonance Imaging Protocol

MRI images were acquired using either a 1.5T (Ingenia; Philips, Best, the Netherlands) or a 3T scanner (SIGNA Architect; General Electric Healthcare, Milwaukee [WI], United States) with 20- and 32-channel head coils, respectively. The ZTE MRA can only be acquired in the 3T scanner. MRA scan parameters are listed in the Table.

DSA was performed using a biplane angiography system (Allura Xper FD 20/20; Phillips, Amsterdam, the Netherlands, and ARTIS icono biplane; Siemens, Erlangen, Germany), under local anaesthesia and using femoral arterial access.

Case 1

A 59-year-old woman who presented with a left-sided third cranial nerve palsy was diagnosed with a left-sided direct-type CCF and a left supraclinoid ICA saccular aneurysm on DSA. Both were treated simultaneously with placement of a flow diverter in the segment of vessel from the cavernous ICA to the middle cerebral artery, with additional transvenous coil packing in the left cavernous sinus. She was noted to have residual CCF on follow-up DSA. On MRI, TOF MRA image (Figure 1a) showed coil-related magnetic susceptibility artefacts in the left cavernous sinus, which obscured the signal around the left ICA. ZTE MRA (Figure 1b and 1c) more clearly depicted abnormal extra-stent signal in the left cavernous sinus, corresponding to the residual CCF, and abnormal flow signal in the left pterygoid plexus, which correlated with the venous drainage on DSA (Figure 1d).

Case 2

A 55-year-old woman presented with left 6th and

Table. Relative comparison of common cerebral magnetic resonance angiography techniques.

	Need for IV contrast	Scan time	Spatial resolution	Temporal resolution	AVF/AVM visualisation
TOF MRA	-	++	++++	-	++
ZTE MRA	-	++++ (longest)	+	-	+++
Phase contrast MRA	-	+++	+++	-	+
CE-MRA	+	+(shortest)	++	++++	+++

Abbreviations: AVF = arteriovenous fistula; AVM = arteriovenous malformation; CE-MRA = contrast-enhanced magnetic resonance angiography; IV = intravenous; MRA = magnetic resonance angiography; TOF = time-of-flight; ZTE = zero echo time.

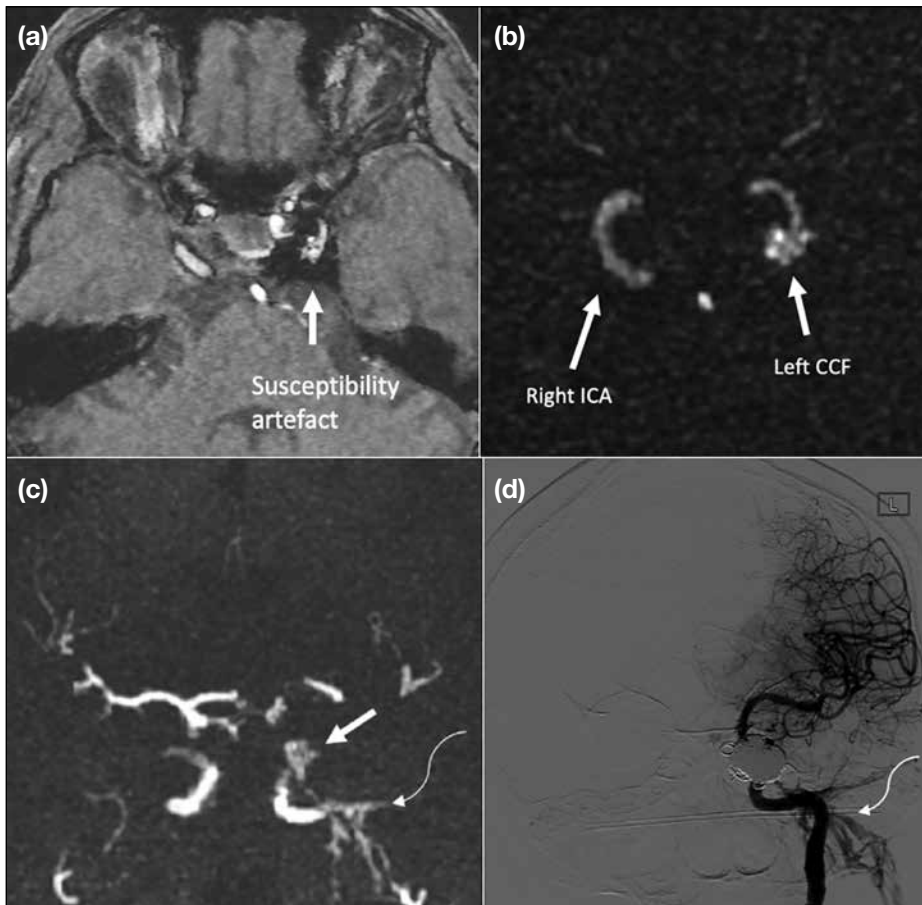


Figure 1. Case 1. Time-of-flight magnetic resonance angiography (MRA) image (a) showing susceptibility artefacts around the flow diverter (arrow). Zero echo time (ZTE) MRA image (b) clearly showing abnormal extra-stent flow signals in the left cavernous sinus, confirmed to be residual left direct carotid cavernous fistula (CCF) on digital subtraction angiography (DSA). A coronal reformat of maximum intensity projection ZTE MRA (c) shows the residual left CCF (straight arrow) and drainage into the left pterygoid plexus (curved arrow). Corresponding DSA image (d) also shows the drainage into the left pterygoid plexus (curved arrow). Abbreviation: ICA = internal carotid artery.

12th cranial nerve palsies. TOF MRA demonstrates heterogeneous flow signal within an abnormally dilated left condylar confluence (Figure 2a) and subtle flow signal around the left vertebral artery (Figure 2b). ZTE MRA more clearly depicts abnormal arterialed flow within the left condylar confluence (Figure 2d) and pronounced asymmetry in the left vertebral artery region, secondary to arterialed flow signal in the venous plexus surrounding the left vertebral artery (Figure 2e). ZTE MRA additionally showed abnormal signal in the left cavernous sinus and superior ophthalmic vein, which was suspected to be concomitant CCF (Figure 2f), with a differential diagnosis of retrograde flow from the condylar dural AVF. The abnormality in the left superior ophthalmic vein is not visible on TOF images (Figure 2c). DSA confirmed both the left condylar confluence dural AVF (Figure 2h) and concurrent left CCF (Figure 2g).

Case 3

A 62-year-old man presented with dizziness. DSA revealed a dural AVF over the right occipital region, with arterial feeders from the right external carotid

artery and the right vertebral artery, and venous drainage into the right sigmoid sinus with retrograde flow to the right transverse sinus. Transvenous embolisation was subsequently performed with complete occlusion of the dural AVF angiographically. Follow-up MRA (Figure 3a and 3b) showed evidence of recurrence of the dural AVF. Both TOF and ZTE MRA showed hypertrophied feeding arteries in the right occipital region and flow signal within the right sigmoid sinus suggestive of arteriovenous shunting. ZTE MRA shows additional retrograde flow signal in the left transverse sinus. A second DSA (Figure 3c) confirmed the recurrent dural AVF and a second transvenous embolisation procedure was performed.

Case 4

A 69-year-old man presented with acute haemorrhage in the left temporooccipital region. DSA showed evidence of dural AVF in the left occipital region, with an arterial feeder from the left occipital artery, and venous drainage into the left sigmoid sinus, left inferior petrosal sinus, and left internal jugular vein. The patient

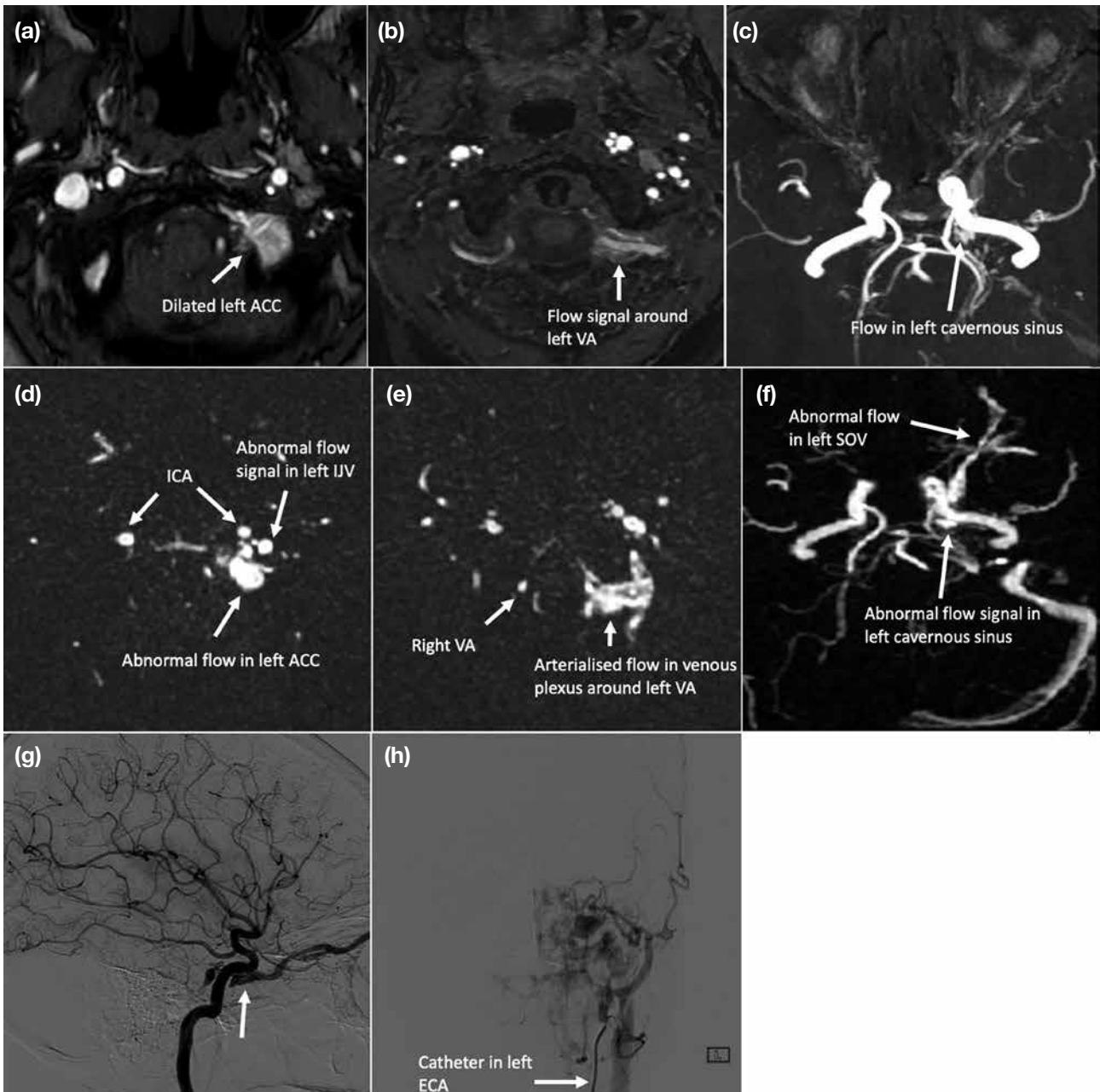


Figure 2. Case 2. Time-of-flight magnetic resonance angiography (MRA) [a-c] demonstrates an abnormally dilated left condylar confluence with heterogeneous flow signal (a) [arrow] and subtle flow signal around the left vertebral artery (b) [arrow]. Zero echo time (ZTE) MRA (d-f) clearly showing abnormal arterialised flow within the left condylar confluence (d) and in the venous plexus surrounding the left vertebral artery (e). Additional abnormal signal in the left cavernous sinus and superior ophthalmic vein, which are more clearly shown on ZTE MRA (f), raises suspicion of concomitant carotid cavernous fistula (CCF) or retrograde flow from the condylar dural arteriovenous fistula (AVF). Lateral digital subtraction angiography (DSA) image (g) on left internal carotid artery injection confirms the concomitant left CCF with drainage into the superior ophthalmic vein (arrow). Frontal DSA image (h) on left external carotid artery injection showing the left condylar confluence dural AVF.

Abbreviations: ACC = anterior condylar confluence; ECA = external carotid artery; ICA = internal carotid artery; IJV = internal jugular vein; SOV = superior ophthalmic vein; VA = vertebral artery.

declined embolisation and elected to undergo imaging surveillance. TOF MRA showed subtle abnormal flow signal in the left sigmoid sinus (Figure 4a and 4b) which was unmistakable on the ZTE MRA (Figure 4c and

4d) and more convincing of arteriovenous shunting. Furthermore, ZTE MRA demonstrated venous drainage to the left inferior petrosal sinus (Figure 4d), which could not be appreciated on TOF MRA image.

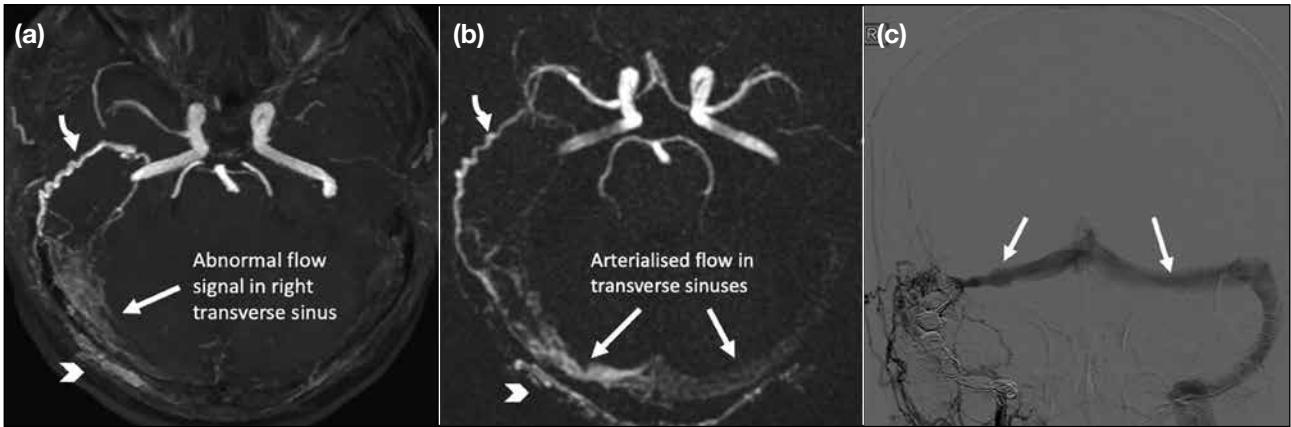


Figure 3. Case 3. Time-of-flight magnetic resonance angiography (MRA) [a] showing abnormal flow in the right transverse sinus (arrow), while zero echo time MRA (b) showing arterialised flow in both transverse sinuses (arrows). Note the arterial feeders from the right posterior auricular (curved arrows in [a] and [b]) and occipital arteries (arrowheads in [a] and [b]). Anteroposterior digital subtraction angiography image (c) after right external carotid artery injection confirms the dural arteriovenous fistula, with drainage into both transverse sinuses (arrows).

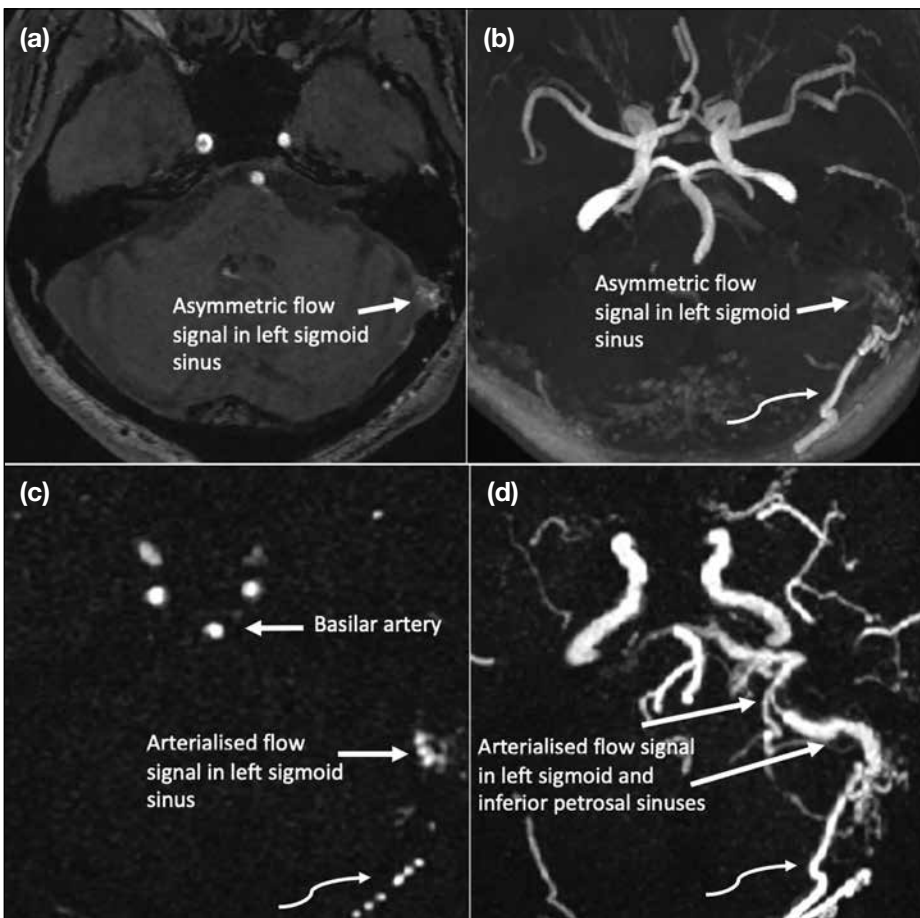


Figure 4. Case 4. Time-of-flight magnetic resonance angiography (MRA) [a, b] showing subtle abnormal flow signal in the left sigmoid sinus (arrows), which was unmistakable on zero echo time (ZTE) MRA (c, d) and more convincing of arteriovenous shunting. The ZTE MRA maximum intensity projection image (d) additionally depicts drainage into the left inferior petrosal sinus. Note the dilated left occipital arterial feeder (curved arrows in [b] to [d]).

Case 5

A 27-year-old woman presented with left occipital lobe haematoma. Investigation with MRA (Figure 5) showed prominent vasculatures and possible nidus at the left

occipital region, suspicious of an underlying AVM. TOF MRA showed a prominent vessel in the region which was more conspicuous in the ZTE MRA, owing to background signal suppression of the technique.

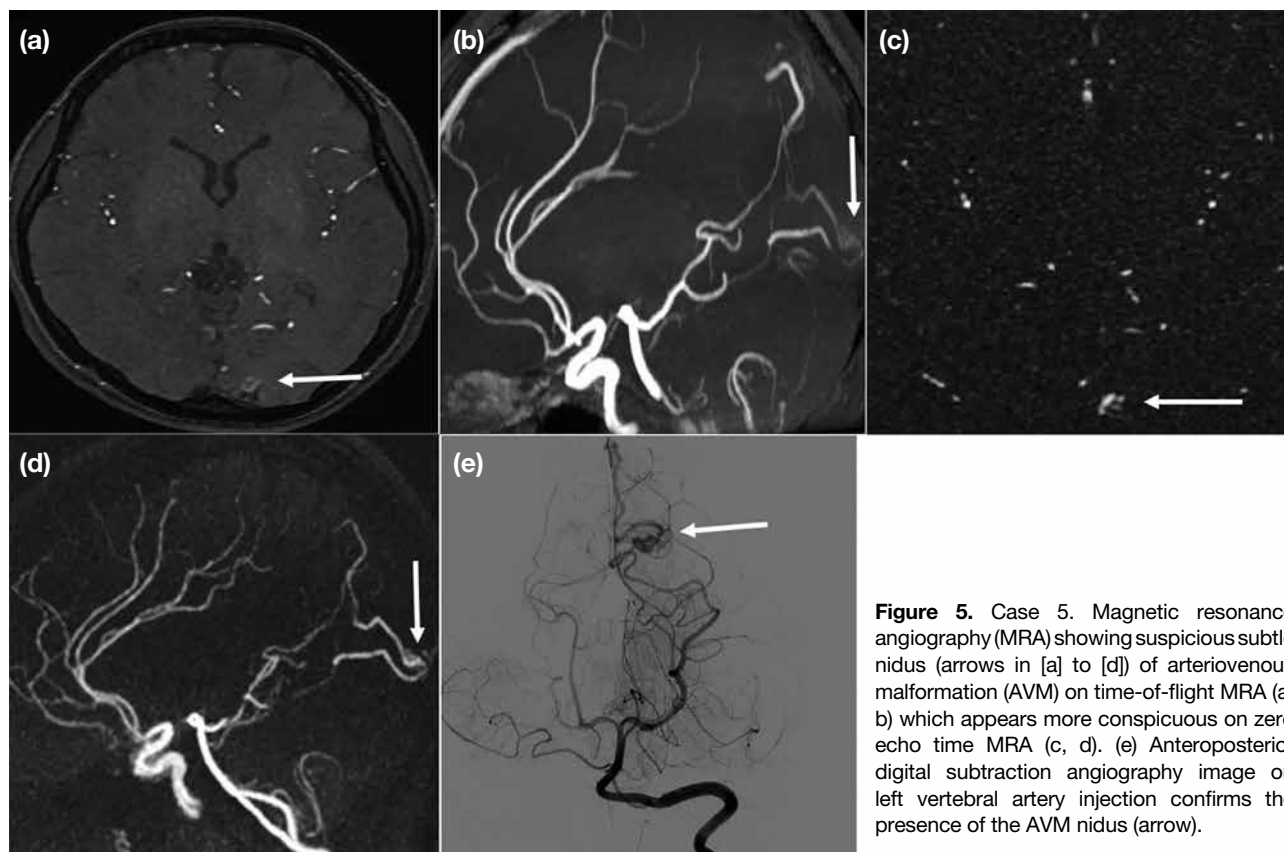


Figure 5. Case 5. Magnetic resonance angiography (MRA) showing suspicious subtle nidus (arrows in [a] to [d]) of arteriovenous malformation (AVM) on time-of-flight MRA (a, b) which appears more conspicuous on zero echo time MRA (c, d). (e) Anteroposterior digital subtraction angiography image on left vertebral artery injection confirms the presence of the AVM nidus (arrow).

Subsequent DSA (Figure 5e) confirmed a small left occipital AVM, with arterial feeder from left posterior cerebral artery and early venous drainage into superior sagittal sinus. The patient was treated with transarterial embolisation.

Case 6

A 53-year-old woman presented with headache. DSA showed an AVM over the left parieto-occipital region, with multiple arterial feeders from the left anterior cerebral artery, middle cerebral artery, and posterior cerebral artery and early venous drainage into the superior sagittal and transverse sinuses. Two-stage treatment was performed with embolisation of the left PCA and subsequent radiosurgery. A small residual nidus was noted on follow-up DSA. Further imaging surveillance was performed with MRA, in which TOF MRA showed subtle flow signal in the left parieto-occipital region (Figure 6a), likely corresponding to the residual nidus. The abnormality was more clearly manifested on ZTE MRA (Figure 6b).

DISCUSSION

We demonstrated the utility of ZTE MRA in the initial

and follow-up evaluation of patients with cerebrovascular malformations. In particular, ZTE MRA allowed for a more confident diagnosis and better characterisation of CCFs, dural AVFs, and AVMs. The imaging was not constrained by artifacts from prior embolisation or stenting. While most arteriovenous shunts could be depicted on TOF MRA, occasionally, the abnormal flow signals may be subtle, and ZTE MRA provided additional strong supporting evidence to proceed to DSA for final confirmation.

TOF MRA relies on the in-flow enhancement effect for detection of signal and is dependent on the alignment of vessels relative to the scan plane. If the direction of flowing blood is parallel to the scan plane, the spins are exposed to repetitive excitation pulses and the flow signal may be saturated and lost.⁹ It is also prone to magnetic susceptibility artefacts and may demonstrate artefactual flow signal in normal venous structures.

In ZTE MRA, the ZTE nature minimises the sensitivity to magnetic field heterogeneity and the phase dispersion of the labelled blood flow signal, hence decreasing magnetic susceptibility artefacts.¹⁰ The ASL technique

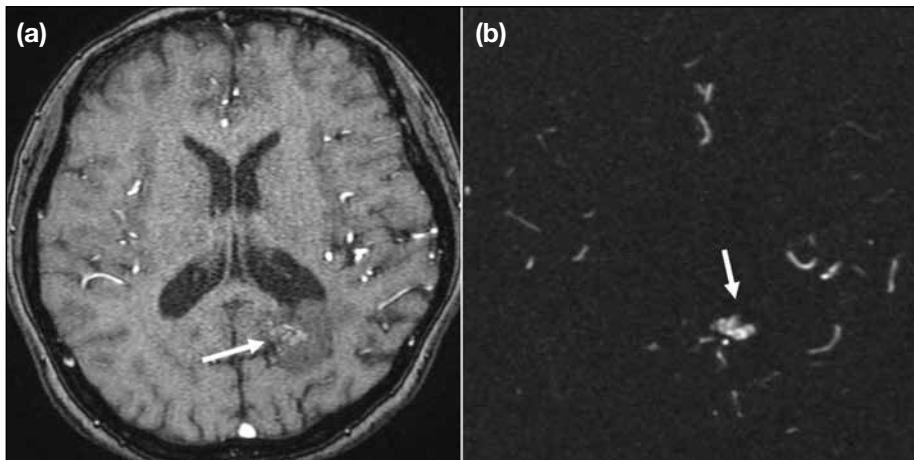


Figure 6. Case 6. Time-of-flight magnetic resonance angiography (MRA) showing subtle flow signal in the left parieto-occipital region (a) which is clearly manifested on zero echo time MRA (b), suggestive of residual arteriovenous malformation nidus (arrows).

uses the water molecules within arterial blood as an endogenous tracer. Hence, it is less influenced by the blood flow state and is not affected by the blood flow direction. The ultrashort echo time acquisition is a defining feature of ZTE MRA that differentiates it from other ASL-based MRA methodologies.

In normal circumstances, venous structures are not expected to show a signal in ZTE MRA because only the protons in the arteries are magnetically labelled. Hence, the signal detected in these vascular regions would suggest underlying arteriovenous shunting. This, too, allows for easier image interpretation.

The background suppression achieved with ZTE MRA also increases the sensitivity of detecting abnormal flow against a dark background. In this sequence, ASL is used as a preparation pulse. A control image is first obtained before the labelling pulse and the labelled image is acquired subsequently. Subtraction of the unlabelled from the labelled images generates the angiographic images and achieves background suppression.¹¹ Our experience highlights such advantage, with abnormal flow signals being more conspicuous on ZTE than TOF MRA, allowing for their easy detection and straightforward interpretation. Furthermore, the ZTE pulse sequence minimises gradient switching, resulting in a quieter scan, which could potentially improve patients' comfort during the examination.¹²

ZTE MRA is not without disadvantages, however. First, it requires longer imaging time (~6 mins vs. ~3 mins for TOF) and thus is theoretically more susceptible to

motion artefact. However, from our experience, most patients were able to tolerate the prolonged acquisition. Second, it has slightly lower spatial resolution due to greater slice thickness and larger pixel size. Further, the low background signal may lead to reduced anatomical information as background structures are not well delineated. In addition, ZTE MRA does not allow vessel selectivity or time-resolved acquisition as in other ASL-based MRA techniques, which could enhance shunt characterisation; however, it still provides a robust screening method prior to reference standard DSA. Finally, ZTE MRA is limited by scanner and hardware availability.

CONCLUSION

ZTE MRA is a useful adjunct to TOF MRA and has good concordance with DSA, potentially obviating the need for CE-MRA. ZTE MRA allows for easier recognition of abnormal vascular shunts, increasing confidence in making the diagnosis as well as improving the characterisation of cerebrovascular malformations.

REFERENCES

1. Morelli, JN, Gerdes CM, Schmitt P, Ai T, Saettele MR, Runge VM, et al. Technical considerations in MR angiography: an image-based guide. *J Magn Reson Imaging*. 2013;37:1326-41.
2. Watanabe K, Kakeda S, Watanabe R, Ohnari N, Korogi Y. Normal flow signal of the pterygoid plexus on 3T MRA in patients without DAVF of the cavernous sinus. *AJNR Am J Neuroradiol*. 2013;34:1232-6.
3. Shang S, Ye J, Dou W, Luo X, Qu J, Zhu Q, et al. Validation of zero TE-MRA in the characterization of cerebrovascular diseases: a feasibility study. *AJNR Am J Neuroradiol*. 2019;40:1484-90.
4. Shang S, Ye J, Luo X, Qu J, Zhen Y, Wu J. Follow-up assessment of coiled intracranial aneurysms using ZTE MRA as compared

- with TOF MRA: a preliminary image quality study. *Eur Radiol.* 2017;27:4271-80.
5. Takano N, Suzuki M, Irie R, Yamamoto M, Teranishi K, Yatomi K, et al. Non-contrast-enhanced silent scan MR angiography of intracranial anterior circulation aneurysms treated with a low-profile visualized intraluminal support device. *AJNR Am J Neuroradiol.* 2017;38:1610-6.
 6. Oishi H, Fujii T, Suzuki M, Takano N, Teranishi K, Yatomi K, et al. Usefulness of silent MR angiography for intracranial aneurysms treated with a flow-diverter device. *AJNR Am J Neuroradiol.* 2019;40:808-14.
 7. Balasubramanian AP, Kannath SK, Rajan JE, Singh G, Kesavadas C, Thomas B. Utility of silent magnetic resonance angiography in the evaluation and characterisation of intracranial dural arteriovenous fistula. *Clin Radiol.* 2021;76:712.e1-8.
 8. Kandasamy S, Kannath SK, Enakshy Rajana J, Kesavadas C, Thomas B. Non-invasive angiographic analysis of dural carotid cavernous fistula using time-of-flight MR angiography and silent MR angiography: a comparative study. *Acta Radiol.* 2023;64:1290-7.
 9. Azuma M, Hirai T, Shigematsu Y, Kitajima M, Kai Y, Yano S, et al. Evaluation of intracranial dural arteriovenous fistulas: comparison of unenhanced 3T 3D time-of-flight MR angiography with digital subtraction angiography. *Magn Reson Med Sci.* 2015;14:285-93.
 10. Ryu KH, Baek HJ, Moon JI, Choi BH, Park SE, Ha JY, et al. Usefulness of noncontrast-enhanced silent magnetic resonance angiography (MRA) for treated intracranial aneurysm follow-up in comparison with time-of-flight MRA. *Neurosurgery.* 2020;87:220-8.
 11. Irie R, Suzuki M, Yamamoto M, Takano N, Suga Y, Hori M, et al. Assessing blood flow in an intracranial stent: a feasibility study of MR angiography using a silent scan after stent-assisted coil embolization for anterior circulation aneurysms. *AJNR Am J Neuroradiol.* 2015;36:967-70.
 12. Ljungberg E, Damestani NL, Wood TC, Lythgoe DJ, Zelaya F, Williams SC, et al. Silent zero TE MR neuroimaging: current state-of-the-art and future directions. *Prog Nucl Magn Reson Spectrosc.* 2021;123:73-93.